Applied Geography 98 (2018) 9–21

Contents lists available at ScienceDirect

Applied Geography

journal homepage: www.elsevier.com/locate/apgeog

3-D reconstruction of an abandoned montane reservoir using UAV photogrammetry, aerial LiDAR and field survey

Jakub Langhammer*, Bohumír Janský, Jan Kocum, Robert Minařík

Charles University, Faculty of Science, Department of Physical Geography and Geoecology, Albertov 6, Prague 2, 128 43, Czech Republic

ARTICLE INFO

Keywords:
UAV
LiDAR
Total station
DEM
Bathymetry
Reservoir
Retention

ABSTRACT

The small reservoirs in the European montane landscape, which were built in past centuries for various purposes, represent specific cultural and technical heritage but also feature retention potential for mitigating the emerging impacts of climate change, namely, the course of flooding or droughts. However, the frequent lack of technical data on these historical structures, including their storage volume and flooded areas, prevents their consideration in water management planning.

In this study, we used unmanned aerial vehicles (UAVs) to produce a detailed 3-D reconstruction of an abandoned montane reservoir that was built for timber flowing in the beginning of 19th century and that has not recently been used for any purpose. The UAV imaging and photogrammetric processing provided an ultra-high-resolution 3-D model of the reservoir basin (5 cm per pixel). Bathymetric analyses were performed based on this basin model to calculate the reservoir volume and flooded area for different water levels. The reliability of the UAV-based model was tested by comparing the results with those of elevation models derived from geodetic field survey using a total station and from conventional data sources based on available aerial LiDAR data. The data were compared to the historical estimates of the reservoir parameters found in the literature.

Bathymetric reconstruction of the reservoir properties based on high-resolution UAV data revealed significant retention potential of the structure and historical underestimation of its capacity. The highly detailed UAV-based model helped to eliminate inaccuracies, resulting from the use of the generalized conventional elevation data, that affect the volumetric estimates in the flat topography of the reservoir basin. The study demonstrated the potential applicability of UAV technology for rapid and reliable reconstruction of landscape structures, which is significant for water management.

1. Introduction

The emerging impact of climate change on the alteration of the hydrological regime (Hanel, Vizina, Máca, & Pavlásek, 2012) and the occurrence and impact of hydrometeorological extremes in past two decades highlight the importance of designing efficient mitigation and adaptation measures. A sensible balance between water management and nature conservation is a primary issue in montane basins, affecting the scope of the potential mitigation measures (Lindner et al., 2010; Räsänen et al., 2018). The montane regions in the cultural landscape of Europe feature historical reservoir structures that were built in past centuries for different purposes, including drinking water supply, irrigation, hydroelectric power generation (Wohl, 2006) and, as in the case of Sumava Mts., timber transport (Jansky, 2006). Most of these structures were recently abandoned and are considered to be part of the historical and technical heritage; nevertheless, the reservoirs maintain their retention potential (Kubinsky, Weis, Fuska, Lehotsky, & Petrovic, 2015; Vlček, Kocum, Šefrna, Janský, & Kučerová, 2012). However, the frequent lack of technical documentation and plans to enable assessment of their volumetric properties has prevented the consideration of implementing such structures into water management plans.

In montane regions, the reservoirs located in headwater areas can be effective in mitigating the emerging effects of climate change by transforming peak flows or stimulating water storage in dry periods. Studies based on long-term observations of hydrological processes indicate a rising vulnerability of Europe to the risk of hydrological extremes in the past three decades (Kundzewicz, Pińskwar, & Brakenridge, 2013). Trends in seasonality and the frequency and spatial distribution of the extremes can be detected on a large scale (Hall et al., 2014). In the geographic context of Central Europe, mountain ranges, which are highly sensitive to changes in boundary climate conditions as well as changes in their environmental status, represent a decisive zone to generate surface runoff during hydrological extremes (Barredo, Lavalle, Roo, & De Roo, 2005; Kundzewicz et al., 2013). Analyses

* Corresponding author.
E-mail address: jakub.langhammer@natur.cuni.cz (J. Langhammer).

https://doi.org/10.1016/j.apgeog.2018.07.001
Received 25 February 2018; Received in revised form 27 June 2018; Accepted 1 July 2018
Available online 05 July 2018
0143-6228/

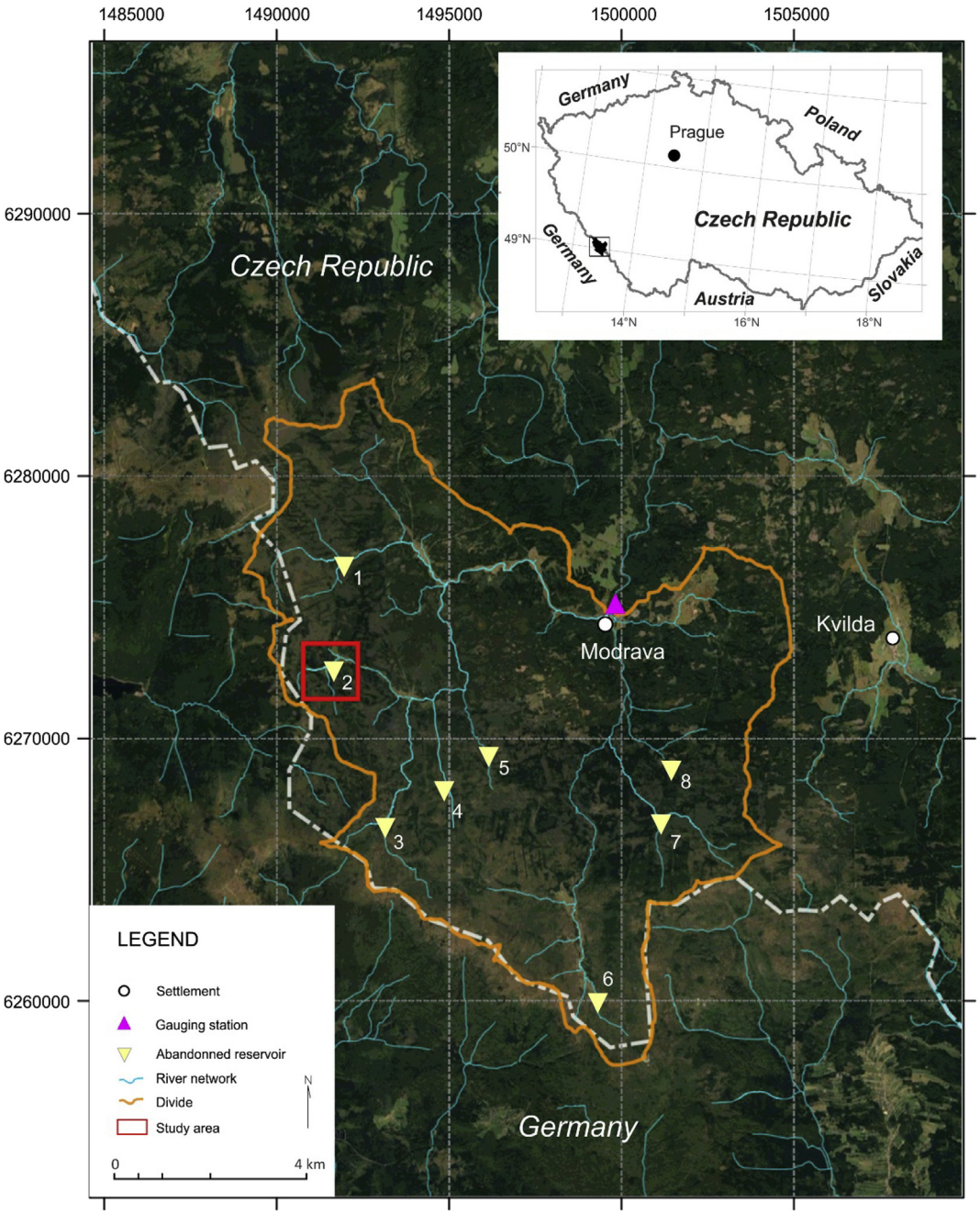

Fig. 1. Study area. Upper Vydra basin, Sumava Mts., Central Europe with the locations of historical timber flowing reservoir marked: 1 - Javoří, 2 - Rokytka, 3 - Roklanská, 4 - Novohuťská, 5 - Studená, 6 - Březník, 7 - Ptačí, 8 - Černohorská.

focused on the long-term trends in the boundary mountains of the Czech Republic (Kliment, Matoušková, Ledvinka, & Královec, 2011; Langhammer, Su, & Bernsteinová, 2015; Vlček et al., 2012) indicated an apparent shift in the frequency and seasonal distribution of floods and the periods of drought over the past two decades.

Our research focused on the abandoned montane reservoirs in the mid-mountain environment of the Sumava Mts., Central Europe. In this area of the Sumava Mountains (Bohemian Forest), a network of montane reservoirs was built in the 19th century to enable timber flowing into lowland regions (Kocum & Janský, 2008). In the second half of the 20th century, the reservoirs were abandoned, and in most cases, their dikes were destroyed.

Due to the long-term gap, there is a lack of detailed historic plans, topographic materials and information on the parameters of the reservoirs, which is a typical phenomenon for the historical landscape reconstructions (Gregory & Healey, 2007). The officially available information for the Rokytka reservoir (NHI, 2015) is based on sparse historical resources that cannot be verified; thus, the past volumetric and areal parameters of the reservoirs should be considered as estimates. Assessments based on field surveys of selected reservoirs (Kocum & Janský, 2008) suggested capacities significantly surpassing historical estimates.

We used UAV imaging as a source of high-resolution spatial data to enable detailed topographic analysis and bathymetric reconstruction of the selected abandoned reservoir structure. Use of UAV photogrammetry enabled 3-D reconstruction of the reservoir structures with an unparalleled level of detail through on-demand data acquisition.

The combination of ultra-high-resolution spatial data with operability in data acquisition is one of the key benefits that UAV platforms brought to the recent development of field survey techniques in

geosciences (Aber, Marzolff, & Ries, 2010; Mišijovský & Langhammer, 2015). The use of programmable unmanned imaging platforms flying at low altitudes revolutionized field survey workflows by delivering high-resolution and accurate 2-D and 3-D spatial information simultaneously (Anderson & Gaston, 2013). Application of UAV in operational surveying results in significantly higher spatial accuracy and acquisition operability than traditional aerial photogrammetry (Tamminga, Eaton, & Hugenholtz, 2015). For applications in hydrology, the key benefit is the ability to build seamless ultra-high-resolution 3-D terrain models of complex segments of stream channels, floodplains or reservoir basins with a level of detail that is sufficient for detailed analysis of runoff and fluvial processes (Flener et al., 2013).

The goals of this study were: (i) to derive the retention volume of the selected reservoir based on UAV survey; (ii) to compare the results with the historical estimates; and (iii) to compare the results achieved using UAV survey with the 3-D reconstructions based on conventional data sources, namely, aerial LiDAR data and geodetic field survey, and to determine their effect on the calculation of the volumetric properties of the reservoir structure to assess the efficiency and potential of the application of UAV imaging and photogrammetry for the reconstruction of historical landscape structures.

We used UAV imaging for accurate 3-D reconstruction of the abandoned reservoir of Rokytka, located at the headwaters of the Sumava Mts. The imagery was acquired by a multirotor platform and was processed to derive a high-resolution DEM of the reservoir basin that was suitable for the identification of even subtle structures in the flat reservoir basin, enabling accurate volumetric calculations. Bathymetric analysis based on the UAV-based model and reference DEMs based on aerial LiDAR scanning and topographic survey were then used to compare the calculated volumetric data with historical estimates.

2. Materials and methods

2.1. Study area

The study site of the Rokytka reservoir (49°00′58.7″N 13°25′02.2″E) is located in the headwater area of the Sumava Mountains, Central Europe (Fig. 1). Historically, this region was covered by virgin forest and peat land, which was replaced in the 18th century by Norway spruce (*Picea abies* [L.] Karst.) monoculture planted for the extensive timber industry (Křenová & Hruška, 2012). To facilitate timber transport from the mountains to the lowlands, where the timber was an in-demand resource for industry, charcoal production, and heating, a complex system of channels and reservoirs was built and used for timber flowing. In the Upper Vydra basin, the system, which was built in 1799–1801, consisted of 8 reservoirs and the Vchynice-Tetov channel connected in a network to enable log transportation (Fig. 1).

Processed wood from the forest stands was transported to the watercourses in winter on sleighs. Wet wood in lengths of 75–100 cm was dried before floating for 2–3 seasons to ease the transport through the shallow riverbeds (Fig. 2b). After World War II, this traditional means of transport was replaced by lifts and trucks travelling the newly constructed access roads. The unused reservoirs were abandoned in the 1960s when the Sumava montane range became a military area along the so-called “Iron Curtain”, a zone with strictly limited access and socio-economic activities along the border between the Czech Republic and Germany. The reservoirs and their remnants remained in the area without use and systematic maintenance until the present (Fig. 2c).

The Rokytka reservoir, representing the study site, was built in the Rokytka (Weitfäller) moorland (Fig. 2a), with a dike crown at an altitude of 1092 m a.s.l. The principal water supply of the reservoir is the headwaters of Rokytka Brook, which drains the montane ridge and forms a natural border between the Czech Republic and Germany. The reservoir is located in the peatland-dominated area in the headwaters of Rokytka Brook, with a catchment of 2.66 km^2. The irregularly shaped reservoir was built in approximately 1800, and according to the available historical records (NHI, 2015), the flooded area reached 1.58 ha with full water storage of 18 000 m^3.

Unlike the other reservoirs in the area, which were destroyed in the second half of the 20th century, the Rokytka reservoir still features a preserved dike with a concrete culvert that enables the potential use of the reservoir for water storage and transformation of peak flows. During flood events, the reservoir works as a dry polder, storing and transforming the flood wave but without the possibility of active control (Fig. 2d).

Due to the gap in socio-economic activity in the military zone during the Cold War era in the second half of the 20th century, which resulted in depopulation and breaks in land ownership, there is a lack of recent historical documents and detailed technical information related to these historical structures. The available information about the retention capacity and the reservoir parameters and operation is fragmented, and the data cited in the literature (e.g.Sumava, 2016) should be considered to be estimates. However, these historical resources suggest that the retention volume of the reservoirs was, with respect to the area of the headwater catchments, considerable, ranging from 1000 to 21000 m^3 (Sumava, 2016).

2.2. Applied methods and data sources

The 3-D reconstruction of the reservoir consisted of the combination of different data acquisition, processing, and analysis techniques. Data sources with different levels of complexity, ranging from the ready-to-use DEM based on aerial LiDAR DEM and the geodetic field survey with further interpolation to the workflow photogrammetric processing consisting of a set of operations, were used, requiring different types of pre-processing before further analysis (Fig. 3).

2.2.1. UAV imaging and photogrammetric processing

The construction of the DEM based on UAV imagery consisted of a set of operations, ranging from physical imagery acquisition, positioning of ground control points (GCPs) and photogrammetric processing, where a point cloud is generated from which the DEM is derived (Fig. 3).

In our study, the UAV imagery was acquired by a multirotor DJI Inspire 1 Pro imaging platform with a Zenmuse X5 camera equipped with a 15 mm prime lens (Fig. 4a). The X5 camera was equipped with 17.3 × 13.0 mm CMOS sensor of micro 4/3 standard with a resolution of 4608 × 3456 pixels (16 Mpix), capturing panchromatic imagery separable to the R-G-B spectral bands. The imagery was taken at an altitude of 91.5 m above ground in compliance with the national UAV flying altitude limit of 300 m and respective regulations (Act No. 49/1997 coll.). During the imaging campaign, which consisted of three flights, 492 images were acquired, all with 70% front and side overlap (Table 1). GNSS was used to capture the GCPs used for georeferencing of the imagery. GCP positioning was performed using a GNSS Topcon HiperSR device operating in real-time kinematics (RTK) mode using the network of permanent CZEPOS GNSS stations managed by the Czech Land Survey Office, enabling centimeter-level accuracy (Fig. 4b). The S-JTSK Krovak (EPSG 2065) coordinate system was used for mapping and geolocation, and two sets of control points were collected for photogrammetric processing. The 16 GCPs used for georeferencing of the imagery were collected first, followed by 9 check points distributed over the study area for photogrammetric processing accuracy control.

Photogrammetric processing of the UAV imagery was performed in the Agisoft PhotoScan Professional 1.3.1. software suite employing the Structure from Motion (SfM) bundle adjustment algorithm (Fonstad, Dietrich, Courville, Jensen, & Carbonneau, 2013). The SfM algorithm enables the use of unstructured imagery for semi-automated alignment and the generation of point clouds (Turner, Lucieer, & Watson, 2012; Westoby, Brasington, Glasser, Hambrey, & Reynolds, 2012). The rapid development in photogrammetric techniques, resulting in algorithms

Fig. 2. Rokytka reservoir. a) Historical map of the reservoir from 1857, b) Timber flowing on a historical postcard, c) Aerial view of the abandoned Rokytka reservoir with a dike crossing the valley, d) Recent status of the reservoir dike with remnants of a culvert.

such as SfM and semi-global matching (Hirschmuller, 2005), has resulted in the availability of user-friendly desktop and cloud-based software tools (Turner, Lucieer, & Wallace, 2014), opening the potential of UAV photogrammetry to the wide area of disciplines in geosciences (van Rees, 2015).

To reconstruct the Rokytka reservoir, the standard photogrammetric workflow in Agisoft Photoscan Pro was applied. The imagery processing consisted of alignment of the imagery (Fig. 4c), sparse and dense point cloud construction, classification of ground points (Fig. 4d), digital elevation model construction (Fig. 4e) and the resulting orthomosaic (Fig. 4f). The input imagery was recorded in jpg file format, and a PC-based workstation equipped with an Intel Core I7-6700, 4.0 GHz, 64 GB RAM and two NVIDIA GeForce GTX980 GPU units was used for the photogrammetric processing.

2.2.2. Field survey and aerial LiDAR data

The DEM developed according to conventional geodetic survey was based on measurements taken by a total station. During a three-day survey campaign, 1118 points were measured using a Leica TCRP1202 R1000 total station. The points were distributed in transverse cross sections throughout the lake basin, perpendicular to the watercourse, and were completed by points distributed along the Rokytka Brook, shaping the basin of the Rokytka reservoir.

The study area was recently covered by aerial LiDAR scanning data, which served as a basis for the nation-wide DEMs provided by the Czech Cadastral Office. The aerial LiDAR scanning campaign that covered the area of the Czech Republic including the study area was launched in 2009–13 with an average data point density of 1–2 points per square meter (Šíma, 2013). The scanning was performed by the LiteMapper 6800 system with a RIEGL LMS – Q680 scanner with autonomous GPS positioning.

From these aerial LiDAR data, the Czech Cadastral Office derived two DEMs with different levels of generalization and spatial resolution: the DMR4G model with 5 × 5 m resolution and launched in 2014 and the DMR5G, featuring 2 × 2 m resolution per pixel and released in 2016. The two datasets feature different spatial resolutions and levels of accuracy. For DMR4G, the vertical error is stated as 0.3 m for open areas and 1 m in forested area; for DMR5G the vertical error is listed as 0.18 m for open areas and 0.3 m in forested areas (Brázdil, 2016). Both DEMs were used in this study as reference elevation datasets.

The available official geospatial data products including the aerial LiDAR data are based on the Czech national coordinate system S-JTSK (EPSG 5514, Krovak East North), representing a national standard for geodetic surveying, mapping and geospatial data products and so this coordinate system was used as a geospatial framework for all spatial data and field survey in this study.

2.2.3. Bathymetric modeling

Modeling of the bathymetric properties and extent of flooded area was performed using the SAGA GIS lake flood module. The algorithm performs flooding of the digital elevation model, starting from the given seed point, and calculates flooding either as relative superelevation over the seed point or as an absolute water level at a given point. In our study, the absolute water level, related to the known elevation of the reservoir dike, was used to calculate the bathymetric properties at different water levels.

The seed point for flooding was located at the reservoir outlet, the lowest known point of the basin, at the former culvert draining the reservoir. The volumetric and areal properties of the flooded area were calculated for a set of water levels, ranging from the dike crown to the altitude at the basin outlet. The bathymetric analysis was conducted in 5 cm intervals across the selected span of water depths. For each water depth, the flooded area and storage volume above the cutting plane were calculated.

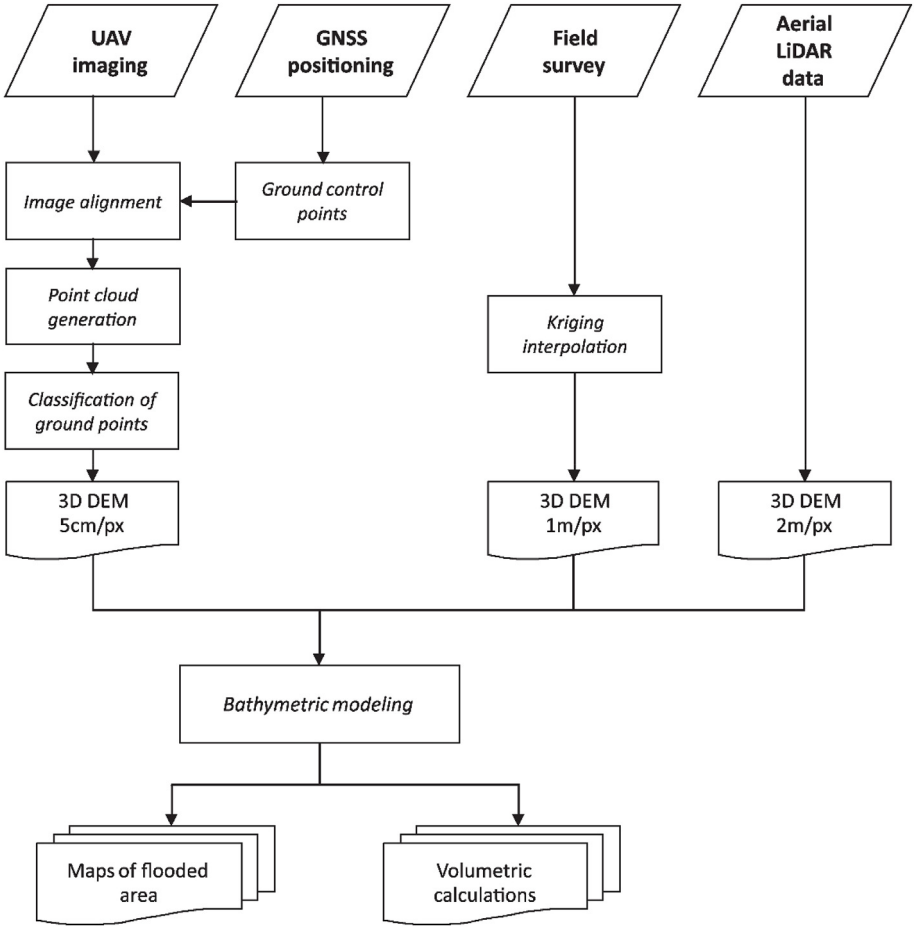

Fig. 3. Workflow of the 3-D reconstruction based on UAV photogrammetry, field survey, and aerial LiDAR data.

3. Results

3.1. 3-D reconstruction of the Rokytka reservoir basin

3.1.1. Reconstruction based on UAV photogrammetry

The photogrammetric reconstruction based on UAV imagery was based on the set of 492 images taken during one imaging campaign in May 2016. The ground resolution of the imagery, given by the flight height and sensor parameter was 2.14 cm per pixel. Based on the imagery taken at an average altitude of 91.5 m above ground, a dense point cloud containing 146.7 million data points was created (Table 1). The dense point cloud was then classified to separate the points representing the ground from those representing vegetation. The Agisoft PhotoScan Dense cloud classification module was used to separate the vegetation with 18.5° as the threshold for the angle and 0.5 m as the distance and cell size used to detect non-ground pixels.

Based on the classified dense point cloud, the DEM was generated with a generic resolution of 4.27 cm per pixel. The elevation model point density was of 547.6 points per m^2 (Table 2). The resulting DEM grid (Fig. 5a) used for further bathymetric modeling was sampled to the size of 5 cm per pixel and consisted of 22.836 million grid fields.

The accuracy of the DEM, checked by calculating differences of Z values at Check Points (CPs). The average difference of the CP altitudes, measured by the GNSS from the generated DEM grid is 7,25 cm (Table 1). The differences of values, both on positive and negative side, are ranging from 1,55 to 11,86 cm (Fig. 5b). The differences of altitude values between the values surveyed by GNSS at GCPs and CPs and the values, measured from the UAV and aerial LiDAR DEMs are listed in detail in the supplementary data, Table S1. The lake, flooded over the UAV-based elevation model at an altitude of 1091 m a.s.l. (Fig. 6), features a maximum depth of 2.81 m and covers an area of 23 896 m^2. The volume of the reservoir according the UAV-based model at this water level altitude is 20 163 m^3.

3.1.2. Reconstruction based on total station measurements

The DEM, based on geodetic survey was built from 1118 points measured by a total station. Based on these points, interpolation using kriging was performed to create a basin model with a grid size of 1 × 1 m^2 (Fig. 7). The DEM grid consists of 370 557 grid fields, representing a point density of 56 points per m^2. Of the total grid fields, only 56 332 represent the potential reservoir basin, delineated by the dike altitude of 1092 m a.s.l.

The maximum depth of the reservoir basin, relative to the dike crown is 3.6 m, corresponding to an area of 56 332 m^2 and a basin volume of 66 232 m^3. However, these parameters represent the geometric properties of the reservoir basin and not the storage potential of the lake. The properties calculated for a water level at an altitude of 1091 m a.s.l. are substantially lower, with a flooded area of 27 948 m^2 and a retention volume of 25 686 m^3.

3.1.3. Reconstruction based on aerial LiDAR data

Both of the conventional DEMs based on aerial LiDAR data were used for the 3-D reconstruction of the reservoir. The DMR4G model, with resolution of 5 × 5 m, and the DMR5G model, with grid resolution of 2 × 2 m, were used to flood the reservoir by use of the SAGA lake flood algorithm.

The reservoir model, based on the DMR5G DEM consists of 53 112 grid fields. The maximum depth of the lake flooded to the water level of 1091 m a.s.l. reaches 3 m with a flooded area of 26 354 m^2. The retention volume of the reservoir based on DMR5G reaches 48 133.20 m^3.

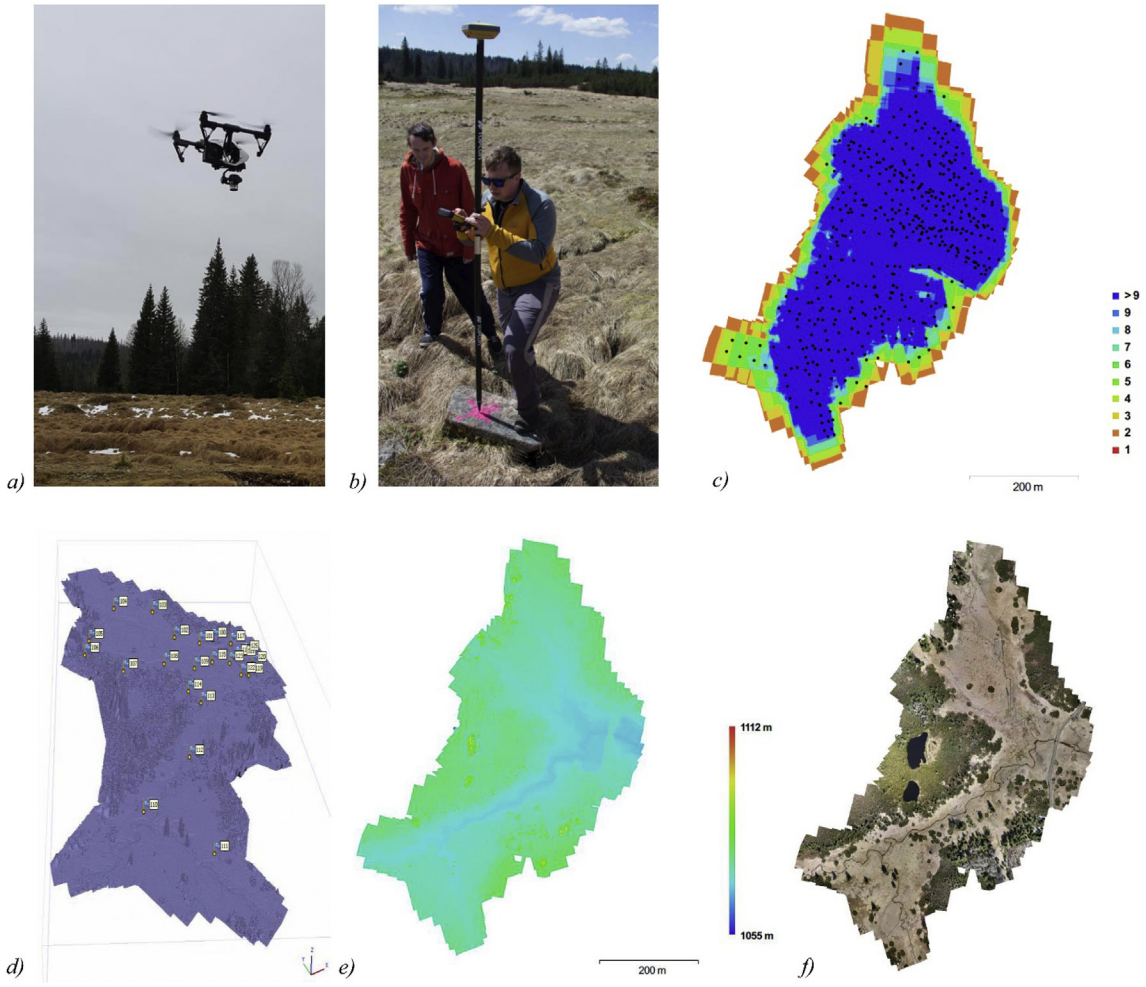

Fig. 4. Key stages and products of the UAV imaging and data processing workflow. a) UAV imaging using the DJI Inspire 1 Pro platform, b) Positioning of the GCPs in the abandoned reservoir basin, c) Alignment and overlap of the imagery, d) Classified dense point cloud, e) Digital elevation model, f) Orthoimage.

Table 1
Photogrammetric processing parameters.

Parameter	*Value*
Flying altitude	91.5 m
Ground resolution	2.14 cm/pix
Coverage area	2.34e + 05 m^2
Camera stations	492
Tie points	4 880 289
Projections	23 233 784
Reprojection error	0.992 pix
Dense Point Cloud: Points	146 678 081
Faces	29 184 787
Vertices	14 603 203
DEM resolution	4.27 cm/pix
DEM point density	547.612 points per m^2
DEM grid size	18 834 × 23 071 pix
Ground Control Points (GCPs)	16
Check Points (CPs)	9
CP mean difference from DEM_{UAV}	7.25 cm
CP minimum difference from DEM_{UAV}	1.55 cm
CP maximum difference from DEM_{UAV}	11.86 cm

The reservoir model based on the DMR4G DEM consists of 8655 grid fields. The lake, flooded to an altitude of 1091 m a.s.l., features the maximum depth of 1.81 m and covers an area of 21 375 m^2, with a retention volume of 15 812 m^3.

Table 2
Bathymetric parameters of the reservoir reconstruction based on flooding the basin derived from different data sources at an altitude of 1091 m a.s.l.

Data source	Number of data points	Field size [m]	Max depth [m]	Mean depth [m]	Flooded area [m^2]	Volume [m^3]
Historical estimate	N/A	N/A	N/A	N/A	26 600	18 000
UAV 5 cm	21 405 266	0.05	2.98	1.07	23 896	20 163
Total station	1118	10	3.6	1.2	27 948	25 686
LiDAR 2 m	53 112	2	3.00	0.23	19 440	15 884
LiDAR 5 m	8655	5	1.81	0.07	19 350	15 812

3.2. Differences among reservoir models based on different data sources

The differences among the four elevation models used for the bathymetric analysis were determined using the control points acquired by RTK GNSS positioning and by cross sections delineated over the reservoir basin (Fig. 8). The analysis indicated significant differences among the models based on data with different point densities, levels of generalization and grid resolutions. Cross sections were placed over the reservoir basin to analyze the distribution of the differences in altitude among the data sources in different parts of the basin (Fig. 8).

All DEMs reliably describe the basic shape of the basin and the distribution of the depth values of the basin, with a good fit of the

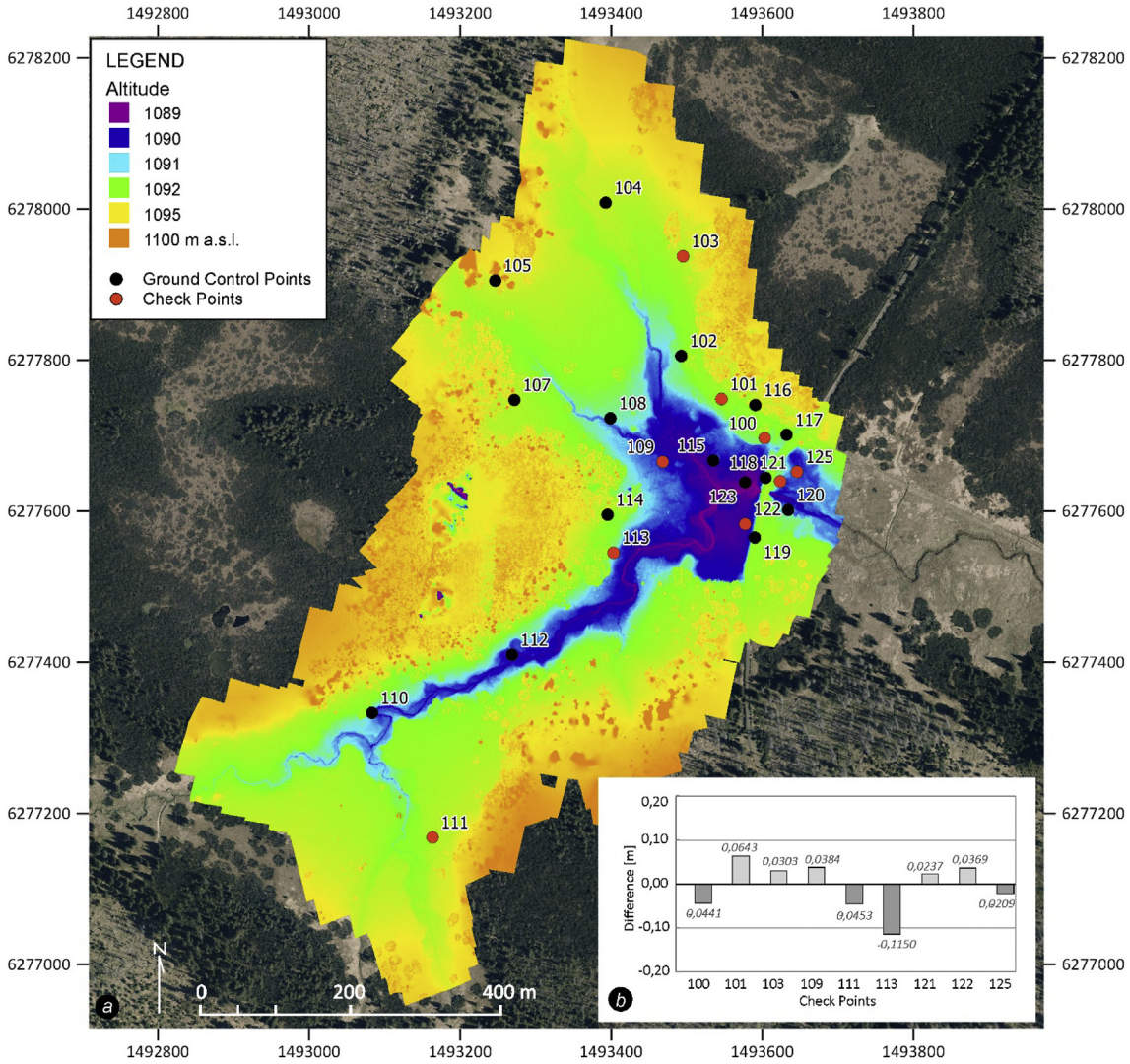

Fig. 5. Rokytka reservoir elevation model based on the UAV photogrammetry. a) 5 cm UAV-based DEM with marked position of Ground Control Points and Check Points. b) Measured differences between UAV-based DSM and the check points.

absolute altitude values of the significant structures of the reservoir, such as the dike, the cross profile along the dike and the longitudinal profile of the key tributaries (Fig. 8). Owing to the different densities of the source data points and the irregular distribution of the total station measurements, there are significant differences in the abilities of the models to describe the inner structure of the reservoir basin formed by a flat and shallow basin with narrow channels.

The cross sections plotted over the reservoir basin show an apparent systematic difference among the data sources. The DEM based on the 5 × 5 m grid DMR4G usually achieves the highest altitude values. The 2 × 2 m DMR5G grid, originating from the same aerial LiDAR data, has a similar distribution of elevation values over flat areas, but differences become apparent in zones with higher variability, such as near the stream channel, at the basin banks and at the edges of the lake.

The DEM based on the total station measurements show the lowest observed values in most cross profiles, including in the central part of the basin, where the difference in some areas reaches almost 0.5 m. In the flat areas, the difference between the model based on the total station measurements and the other DEMs is the highest, with zones with of positive and negative differences.

The UAV data perform best in the reconstruction of the fine structures of the reservoir bottom due to the very high spatial resolution (Fig. 8). The elevation of the lowest parts of the basin (e.g., channels or depressions) in the UAV model mostly matches the values based on the total station survey. On the other hand, in the large flat zones of the basin bottom, the elevation values of the UAV model are more similar to the aerial LiDAR-based models.

These differences might be related to the different nature of the data. The elevation model based on the total station survey is highly reliable for describing the stream channel structures because of the distribution of the data points located along the lowest parts of the basin. Due to the ultra-high resolution of the UAV data, these fine structures are properly reconstructed; however, the LiDAR-based DEMs with grid sizes of 2 and 5 m are too coarse to reliably capture the fine structures of the narrow stream channel. Moreover, the lower values reached by the total station measurements in the flat areas could be a product of the different elevation data acquisition methods. The physical elevation survey measured by a geodetic pole might result in low values due to the adjustment of the pole to the soft soil ground compared to optical scanning of the reservoir basin surface covered by montane grass.

3.3. Bathymetric analysis

The bathymetric analysis of the former Rokytka basin reflects the differences in data of varying origin and level of generalization. Despite

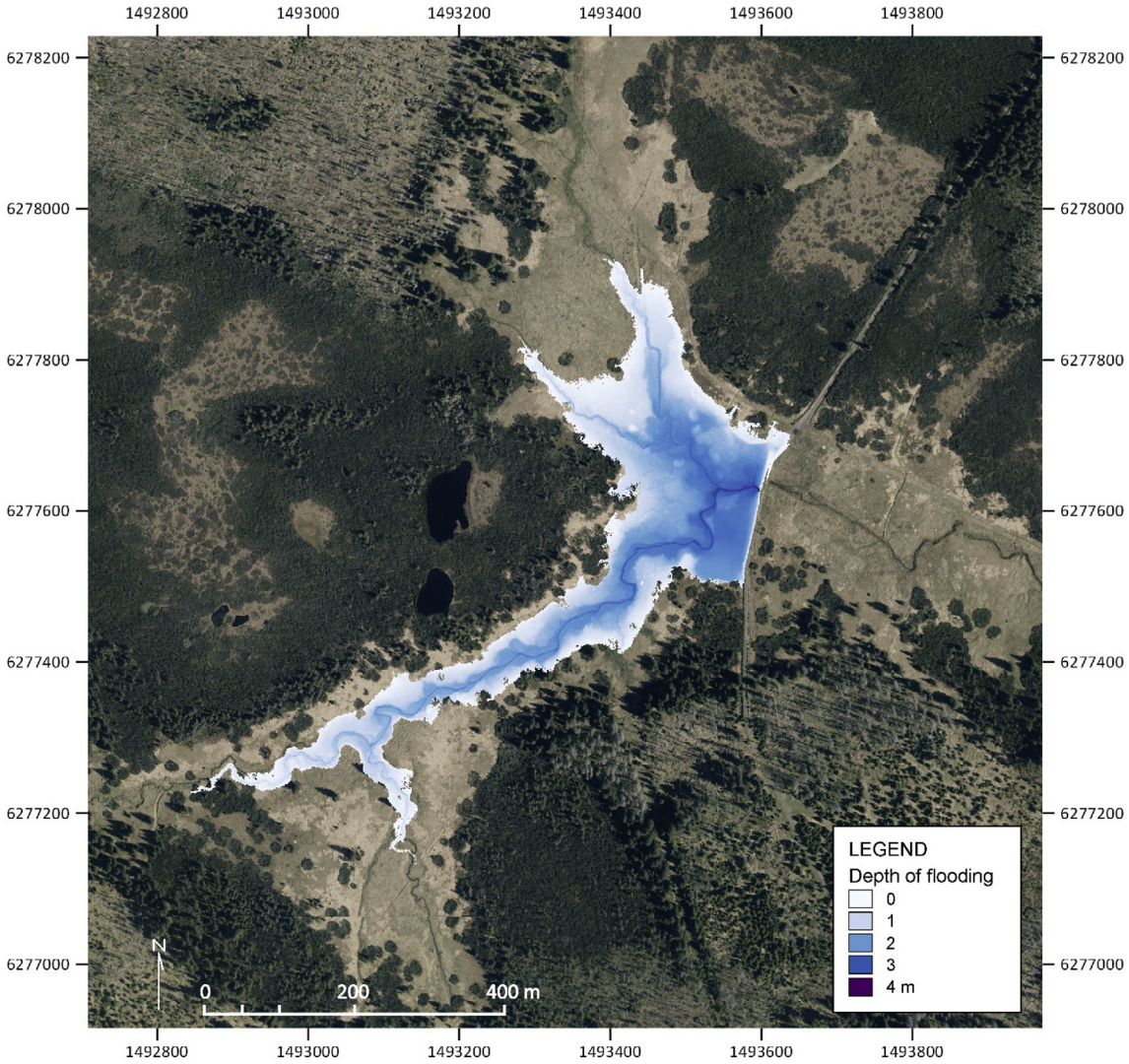

Fig. 6. Rokytka reservoir flood model based on the UAV photogrammetry. Flooding of the basin at 1091 m a.s.l.

the differences, all the models accurately reflect the steep rise in flooded area in the flat and shallow reservoir basin (Fig. 9). However, substantial variability is apparent in the parameters reflecting the variability of the elevation and the level of detail of the reservoir bottom reconstruction, including the parameters of water depth and storage volume, calculated for a given water level.

The maximum water depth in the reservoir when filled to the realistic maximum storage volume at approximately 1 m below the dike crown at 1091 m a.s.l. does not exceed 3 m, except for the model based on the total station measurement. The maximum depth is reached in a very limited zone near the reservoir outlet, and the flooded zone of most of the basin is very shallow. The mean water depth for the models based on the aerial LiDAR data, which do not reflect the channel structure, is extremely low: 23 cm for the 2 m grid and 7 cm for the 5 m grid (Table 2). These differences demonstrate the limited reliability of the estimates based on the generalized data, in particular in the shallow edges.

The effect of the higher level of terrain generalization in the DEMs based on the aerial LiDAR data is apparent in the calculations of the flooded volume and area (Table 2). Despite the differences in geometric resolution and level of generalization, the DEMs based on the aerial LiDAR data produce nearly identical values of storage volume and flooded area (Table 2). The reconstructions based on more detailed data that better describes the inner structure of the reservoir, i.e., the total station and UAV models, produce significantly higher estimates of the storage volume and flooded area (Table 2, Fig. 10).

There is a lack of information on the exact water level used to calculate the storage volume in historical data, leading to difficulties in comparing recent calculations to historical estimates. Based on the available records, descriptions, imagery, and maps, we used a water level of 1091 m as a reference. At this altitude, the water level is 1 m below the reservoir dike crown, which could be considered as a realistic estimate of the planned capacity when taking into account the physical properties of the dike and the culvert size and location. The retention volumes calculated using recent technologies fit the historical records for this water level (Table 2).

For level of flooding of 1091 m a.s.l, corresponding to flooding up to 1 m below the dike crown, the retention volume according to the conventional DEM is approximately 15800 m^3, with a flooded area of 19400 m^2. The calculated volume is thus lower than the historical estimate of 18000 m^3, and the calculated flooded area is significantly smaller than the historical estimate of 26600 m^2.

Compared to the conventional DEM, the 3-D reconstruction based on the UAV-derived topography indicates higher storage potential. For the given flood level, the retention volume reaches 20163 m^3, which is 22% higher than the model based on the aerial LiDAR data and 11% higher than the historical estimate. The UAV-based model also indicates a larger flooded area, although the difference is less marked than that of

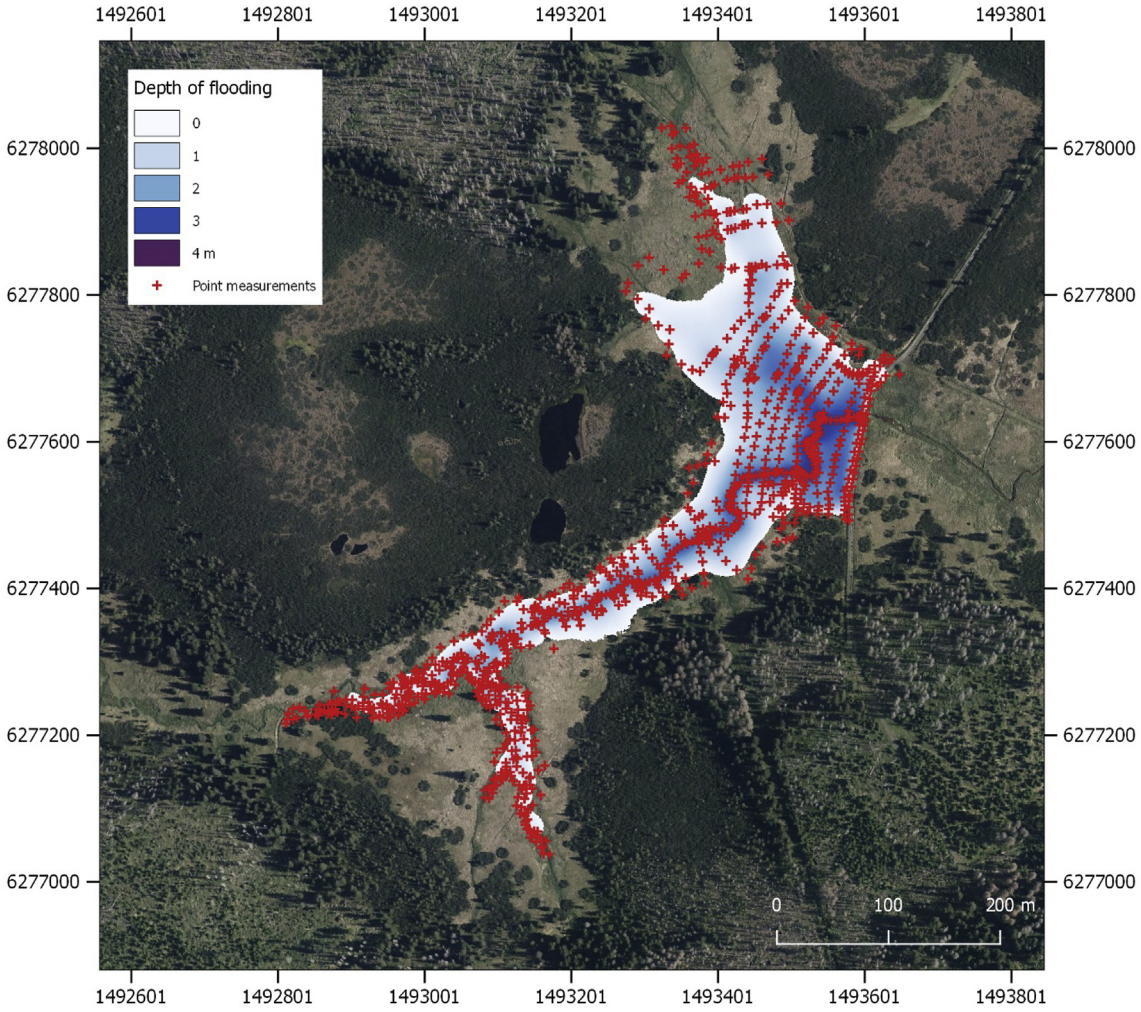

Fig. 7. Rokytka reservoir model based on the geodetic survey with plotted points flooded at 1091 m a.s.l.

the storage volume (Fig. 10).

The above comparison indicated that a higher level of generalization leads to lower estimates of the reservoir retention capacity. The flat shape of the basin results in a steep increase in the storage volume with only a mild rise of the flood water level: an increase in water level of 0.5 m almost doubles the flooded volume (Table 3).

Compared to the results of the models based on aerial LiDAR and UAV data, the bathymetric model based on total station measurements displays substantially high retention volumes. For all water levels, the retention volume significantly exceeds the results from the other data sources, including the UAV terrain model (Table 3).

These results suggest that despite the high accuracy achieved at individual points, the irregular distribution (Fig. 7) and low density of the points (Table 2) compared to the regular grid of values from the aerial LiDAR or UAV photogrammetry, prevent reliable modeling of the whole area of the reservoir basin.

The differences in the calculations based on the different data sources more significantly affect the volumetric model than the calculation of the flood extent (Table 3). The differences are especially pronounced at low levels of flood spill, when a detailed description of the reservoir bottom is crucial to accurately calculate the lake storage volume. At a water level of 1092 m a.s.l., corresponding to full reservoir capacity, the storage volume according to the UAV-derived DEM is 13.8% higher than the results from a 5 m grid. However, at a water level of 1090.5 m a.s.l., corresponding to flooding of just the basin bottom, the difference is 45.3% (Table 3).

4. Discussion

The progress in the availability of high-resolution digital elevation data covering complex areas derived from aerial or satellite remote sensing creates large potential for terrain reconstructions and analysis, which are traditionally based on geodetic field survey. In particular, the high resolution and reliability of DEMs based on aerial LiDAR scanning enabled the use of seamless and accurate elevation data as the basis for a wide range of applications in geosciences. The availability of new high-resolution data products reveals its potential, especially in disciplines related to modeling hydrological risk processes (Papaioannou, Loukas, Vasiliades, & Aronica, 2016; Vozinaki, Morianou, Alexakis, & Tsanis, 2017) or natural hazards (Sampson, Smith, Bates, Neal, & Trigg, 2016; Thomas et al., 2017/2). However, despite the increasing data resolution, application in specific conditions, such as the indicated the tested case of the flat basin with fine channel structures, remains limited.

The sources of limitations vary. The crucial aspects for the applicability of high-resolution topographic data to reconstruct landscape structures are the physical coverage of the study area and the data accessibility. The spatial coverage of the Earth's surface by high-resolution topographic data, mainly based on aerial LiDAR scanning, is rapidly growing; however, it remains limited to select regions, mostly in developed countries (Sampson et al., 2016). In addition to the physical spatial coverage of the study areas, another data accessibility issue is that the high-resolution topographic data are, with some exceptions, available only as expensive commercial products. For some countries

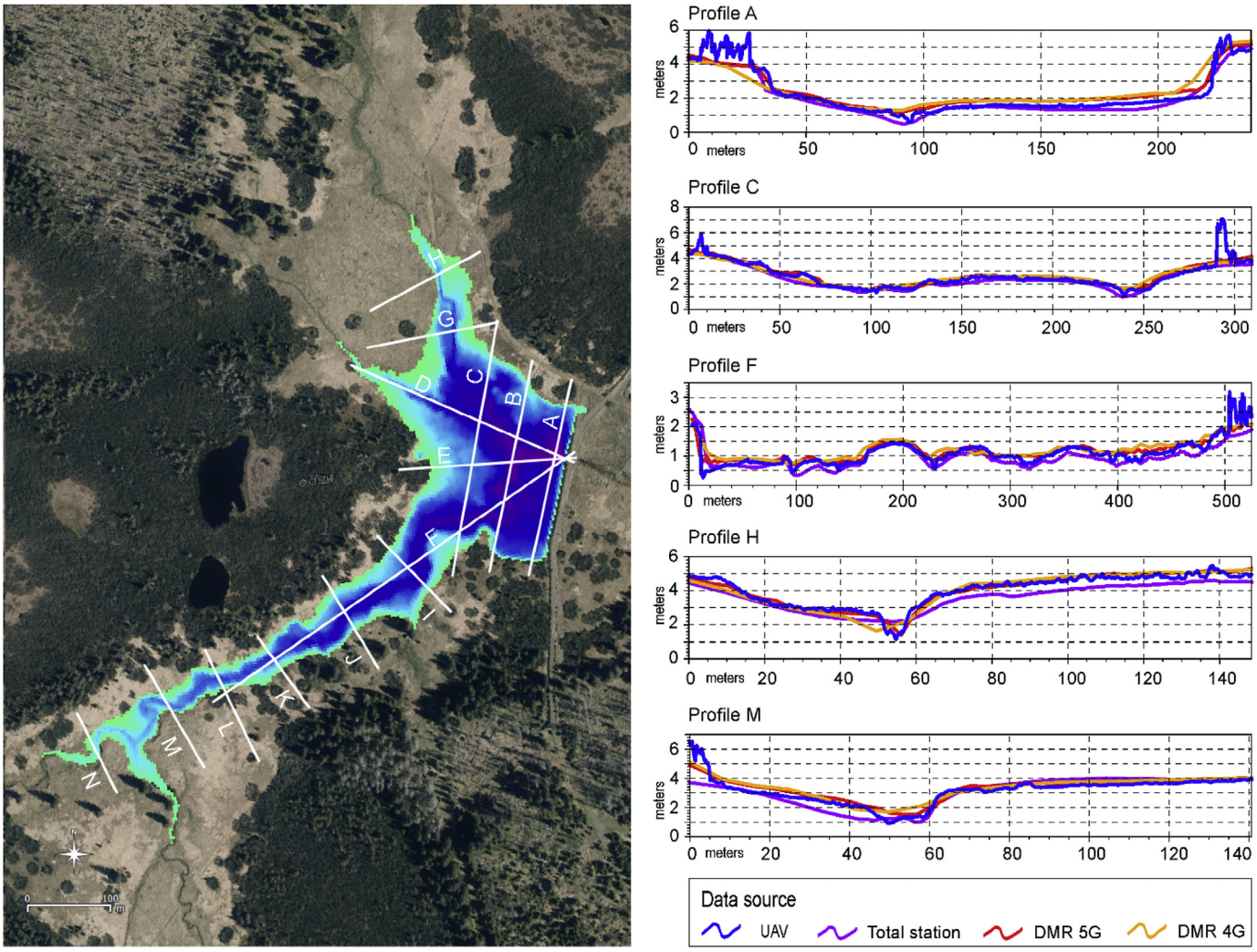

Fig. 8. Cross sections over the reservoir basin with elevation values extracted from the applied digital elevation models.

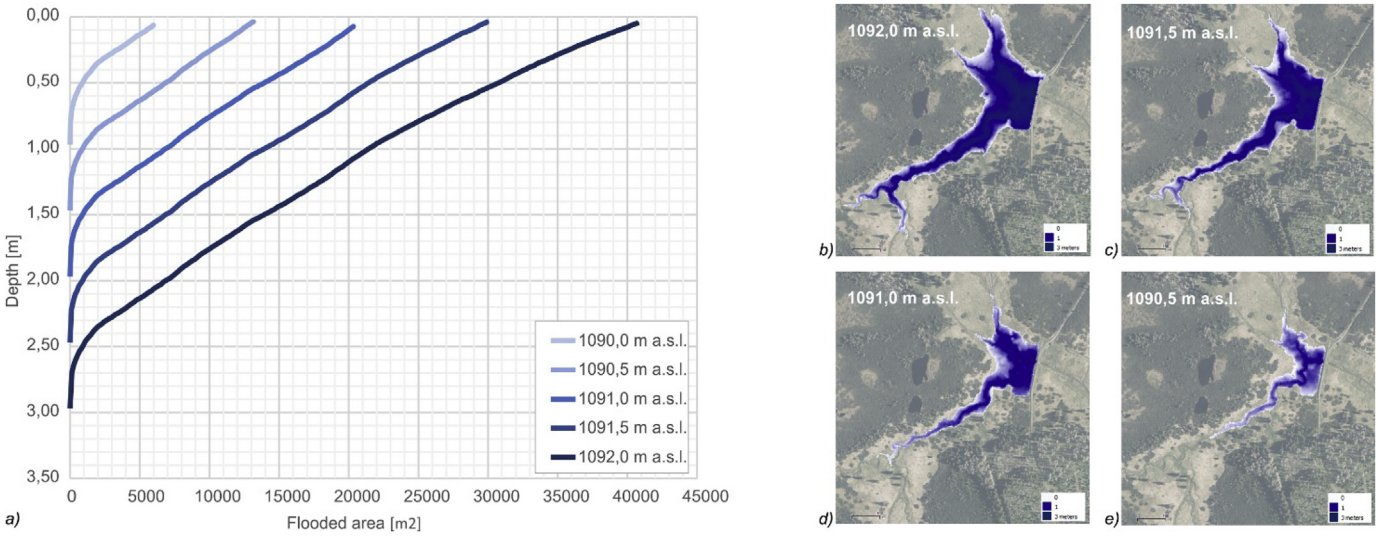

Fig. 9. Flooded area of the Rokytka reservoir at varying water levels based the UAV-based model. a) hypsometric curves for given altitudes. Extent of the flooding at different water levels: b) 1092 m a.s.l., c) 1091.5 m a.s.l., d) 1091 m a.s.l., e) 1090.5 m a.s.l.

and regions, high-resolution topographic data are published as open access data, and there are emerging public repositories of high-resolution topographic data, such as OpenTopography (Crosby, Nandigam, Baru, & Arrowsmith, 2013). However, their coverage remains relatively sparse and spatially inconsistent.

The need for high-resolution data with acquisition operability

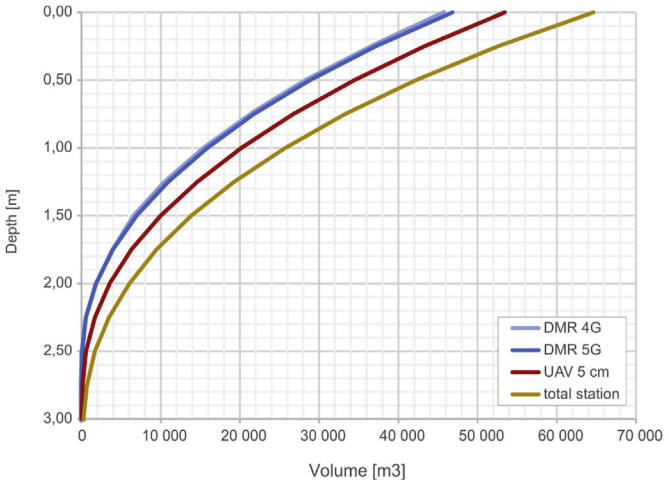

Fig. 10. Bathymetric curve of the Rokytka reservoir based on varying DEM sources: DMR 4G, DMR 5G, total station measurement and UAV photogrammetry.

Table 3
Variability of the reservoir volume, based on the flood level and data source.

Water level [m a.s.l.]	DMR4G volume [m^3]	DMR5G volume [m^3]	Total station volume [m^3]	UAV volume [m^3]
1092.0	46913.4	46838.8	61615.2	53426.9
1091.5	28826.2	28832.3	42191.7	34427.1
1091.0	15812.8	15884.5	25686.2	20163.0
1090.5	6876.0	6958.9	13517.6	9990.5
1090.0	1841.6	1847.2	6048.0	3546.2

creates a niche that UAV technology can fill. In addition to the data acquisition operability, UAV-derived data have proven their ability to achieve spatial resolution significantly beyond conventional topographic data (Fig. 11). The greatest benefit of data with ultra-high resolution on the scale of centimeters per pixel is the ability to correctly represent both natural and artificial fine structures. This ability could play a significant role for hydrological applications, e.g., for hydrodynamic modeling, where the accuracy of riverscape reconstruction is the key to the reliability of the simulation (Kaiglová, Langhammer, Jiřinec, Janský, & Chalupová, 2015).

Similar spatial resolution as by UAVs can be also achieved by low-level aerial imaging, using high-resolution medium format high-resolution cameras, such as Leica ADS40, UltraCamEagle or Phase One (Pepe, Fregonese, & Scaioni, 2018). However, the very high costs of the professional-grade sensing systems and the operating costs of the aerial campaigns makes this approach efficient for applications, requiring large spatial coverage, which is unachievable by UAVs. The high resolution aerial imaging is thus typically used in archeology or urban mapping (i.e. Myeong, Nowak, Hopkins, & Brock, 2001, Pepe & Prezioso, 2016, Tansey, Chambers, Anstee, Denniss, & Lamb, 2009).

The presented case study of the Rokytka reservoir serves as an example. The data density of conventional, high-resolution topographic data is not sufficient to reliably describe the structure of the drainage channels inside the reservoir basin (Fig. 11). This study pointed to substantially different data densities across the data sources. In case of the historical data sources, the number and spacing of original datapoints remains unknown, however, it is assumed to be similar to the recent total station survey. In this campaign, there was collected 1118 points, which results in a density of 0,00048 points per square meter, however, with highly irregular spacing of the initial data points. The DMR 4G and DMR 5G are the official national-wide DEMs with different grid resolution but derived from the same aerial LiDAR scanning source of point density of 1–2 points per square meter (Brázdil, 2016). Most dense data source is then the UAV imaging with in the dense point cloud, derived from the aerial imagery (Table 1) with an average density of 547,6 points per square meter.

Such fine spatial resolution is vital for the accurate estimates of the water storage potential of the structure for the most frequent conditions of low-magnitude flooding, when the unused reservoir could serve as a retention space to transform the flood wave. Even in areas covered by high-resolution conventional elevation data, the application of ultra-high-resolution topographic models derived from UAV imaging could significantly enhance the reliability of the assessment.

The varying accuracy of the 3-D reconstruction, reflected by the differences in the elevation models compared to the surveyed values, is vital to the interpretation of the bathymetric analysis. Comparison of the basin models indicated that the correct description of fine basin structures is most important for a reliable calculation of the retention volume at low levels of flooding, as well as for an accurate assessment

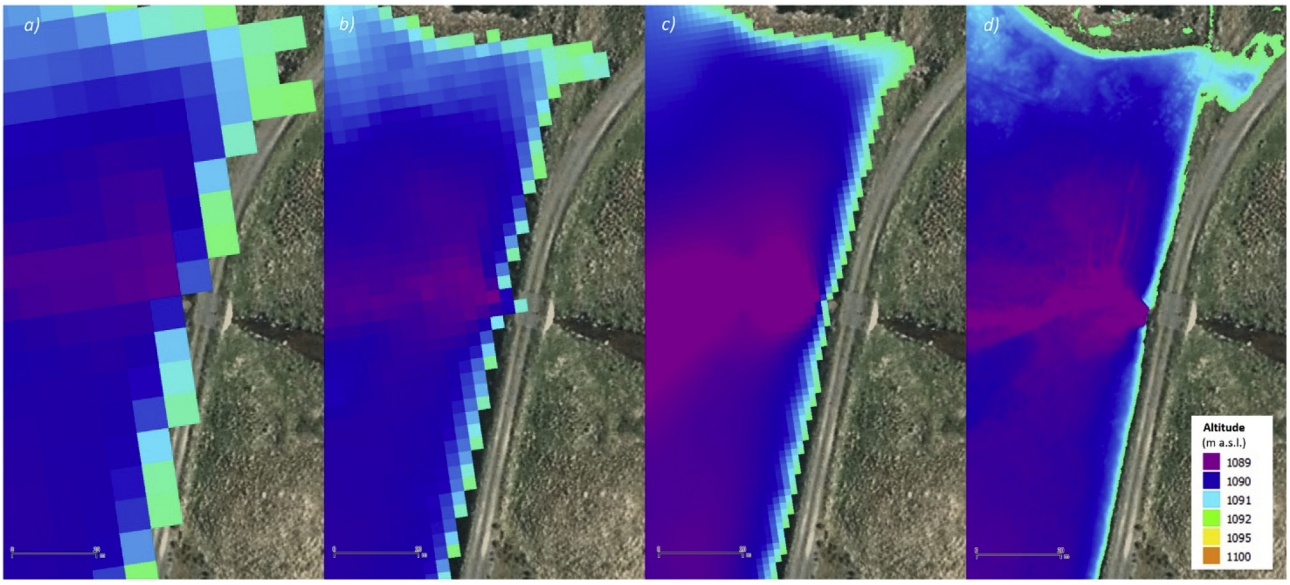

Fig. 11. The effect of the elevation model resolution on the schematization of the lake bathymetry features using the example of the area near the dike crown with different data sources. a) DMR4G (5 × 5 m), b) DMR5G (2 × 2 m), c) total station survey (1 × 1 m), d) UAV imagery (5 × 5 cm).

of the flooded area at the edges of the reservoir basin.

Even the ultra-high-resolution data from UAV photogrammetry are burdened by uncertainty owing to the optical method of information acquisition. Inability to reach beneath vegetation cover remains a persisting problem for the accurate separation of data points representing the surface from those representing the ground (Nex & Remondino, 2014). The point cloud classification methods that are applicable to the detection and separation of distinctive structures, such as trees or buildings, from the ground are inefficient in the case of coverage by low compact vegetation. The height of the grass cover of the montane meadows in the study area, which is dominated by *Carex Rostrata* and *Nardus stricta* L. (Matějková, van Diggelen, Prach, & Marrs, 2003), can reach 20–30 cm, which is significant in the context of the shallow reservoir basin. The montane grass often forms large homogeneous formations with a smooth undulating surface that is difficult to automatically detect and separate from the ground, which remains invisible below the compact cover. In flat terrain, such as in the case of the investigated shallow reservoir basin, a difference in elevation can affect the accuracy of the related volumetric models. However, the shift in elevation resulting from compact grass cover can be reduced by scheduling the imaging campaigns outside of the vegetation season. In our study, we performed the UAV imaging campaign in May, a transition period between the snowmelt and upcoming vegetation season in the montane area.

The 3-D reconstructions based on different data sources, including the latest surveying and photogrammetric techniques, proved the validity of the historical estimates of the reservoir volume. The historical estimates proved to be surprisingly accurate. Despite the accuracy limitations of historical surveying techniques, the lack of detailed topographic maps and the absence of advanced modeling tools, the historical records, in general, fit the volumetric parameters of the reservoir, as apparent from recent measurements.

However, the comparison with the historical estimates should be considered as burdened by uncertainty, resulting from multiple sources. The observed discrepancies between the historical and recently calculated volumetric and area values of the lake flooding can be primarily attributed to the different accuracy, data density and nature of the applied surveying techniques. However, there is also a lack of information on the eventual changes of the reservoir basin properties, i.e. by the siltation or vegetation overgrowth over time. Hence, the comparisons with the historical values should be interpreted with caution and, when available, should be based critical analysis of various data types and sources (Raška & Emmer, 2014).

The bathymetric modeling using high-resolution topographic data revealed that the Rokytka reservoir has higher storage capacity than the historical estimate of 18 000 m^3 (NHI, 2015). The maximum potential storage, corresponding to full capacity of the reservoir (53426 m^3) is triple the retention volume listed in historical records (Table 2). Such volume, however, corresponds to the critical water level hitting the crown of the dike. This level cannot be used as the actual storage volume available for regular water management operations, but it indicates the potential for the mitigation of extreme events.

The Rokytka reservoir, although abandoned, continues to act as a structure that supports the transformation of flood waves, even without direct management or control. An example is illustrated by one of the most significant recent floods in the area, which occurred in December 2015. During this rapid snowmelt flood, an ice jam at the culvert forced temporary water storage with the water level reaching approximately 1.5 m below the dike crown (Fig. 12).

Because the dike culvert is not operated and remains fully open, the reservoir outflow cannot be controlled, and the full storage potential of the dike cannot be applied for efficient flood wave transformation. Even simple control of the water level during critical events could have a substantial effect on water storage. As indicated by the bathymetric analysis (Table 3), an increase in water level by 0.5 m almost doubles the retention volume of the reservoir, which in relation to the relatively small basin, could have significant effects on the transformation of flood waves in the stream system.

Fig. 12. Water level in the reservoir during the flood of December 2015 during the flood culmination.

5. Conclusions

This study aiming to produce a 3-D reconstruction of the abandoned Rokytka reservoir, which was used in the past for timber flowing and currently represents potential retention space for flood control, proved that UAV technology can be used as an efficient and reliable tool to generate highly accurate reconstructions and models of landforms and historical landscape structures.

A 3-D model of the reservoir structure with a resolution of 5 cm per pixel was derived using UAV-based imagery and photogrammetric processing, enabling calculation of the volumetric properties and the extent of flooded area at different water levels. The results were compared with 3-D models based on available aerial LiDAR data with 2 m and 5 m resolution and with a model based on a geodetic survey using a total station.

The bathymetric properties based on UAV photogrammetry enabled construction of a 3-D model that accurately described even the fine structures of the flat bottom of the abandoned reservoir that is formed by a system of narrow and shallow drainage channels. In such conditions, there is an apparent effect of the spatial resolution and generalization, which results in underestimation of the basin volume for the LiDAR-based DEMs and a lack of ability to describe the fine inner structure of the lowest part of the basin. Despite the effect of generalization, the UAV-based and LiDAR-based models report similar altitudes across all zones of the reservoir basin. However, the DEM based on the total station measurements estimates significantly lower altitude values, especially in the central part of the basin, where the difference reaches almost 0.5 m in some areas. The small differences are translated into significantly higher estimates of the basin storage capacity.

The differences are significant, especially in the lowest part of the shallow basin, which is characterized by narrow channels. The varying level of generalization of the spatial information in this zone is then a key source of difference in the resulting bathymetric models, where the differences are more significant in the calculation of the volumetric properties than the flood extent.

Despite the differences among the models, a comparison shows a surprisingly good fit of the historical records. The potential storage capacity of the structure is higher than was estimated in the historical sources: the full capacity of the structure is almost triple the retention volume estimated by the historical records. Although the Rokytka reservoir has been without management and control since the middle of the 20th century, it continues to act as a structure to support the effective transformation of flood waves.

This study proved that the use of high-resolution UAV-based data is of significant importance for the assessment of the actual storage potential of historical landscape structures, which is fundamental information for their potential implementation in water management and flood mitigation plans.

Acknowledgments

This research was supported by the EU COST Action 1306 project LD15130 “Impact of landscape disturbance on the stream and basin connectivity” and by the Czech Science Foundation project 13-32133S “Retention potential of headwater areas”. The authors thank Julius Česák for assistance in geodetic measurements.

Appendix A. Supplementary data

Supplementary data related to this article can be found at http://dx.doi.org/10.1016/j.apgeog.2018.07.001.

References

Aber, J. S., Marzolff, I., & Ries, J. B. (2010). *Small-format aerial photography*.
Act No. 49/1997 coll., On civil aviation and amendment and supplement of act No. 455/1991 coll., on engaging in a trade. Collection of laws 1997, Czech Republic.
Anderson, K., & Gaston, K. J. (2013). Lightweight unmanned aerial vehicles will revolutionize spatial ecology. *Frontiers in Ecology and the Environment, 11*, 138–146.
Barredo, J. I., Lavalle, C., Roo, A. D., & De Roo, A. (2005). European flood risk mapping. *Natural Hazards,* 1–6.
Brázdil, K. (2016). *Technical report to the 5th generation digital terrain model (DMR 5G).* CUZK.
Crosby, C., Nandigam, V., Baru, C., & Arrowsmith, J. R. (2013). OpenTopography: Enabling online access to high-resolution lidar topography data and processing tools. *EGU general assembly conference abstracts* (pp. 13326). .
Flener, C., Vaaja, M., Jaakkola, A., Krooks, A., Kaartinen, H., Kukko, A., et al. (2013). Seamless mapping of river channels at high resolution using mobile LiDAR and UAV-photography. *Remote Sensing, 5*, 6382–6407.
Fonstad, M. A., Dietrich, J. T., Courville, B. C., Jensen, J. L., & Carbonneau, P. E. (2013). Topographic structure from motion: A new development in photogrammetric measurement. *Earth Surface Processes Landforms, 38*, 421–430.
Gregory, I. N., & Healey, R. G. (2007). Historical GIS: Structuring, mapping and analysing geographies of the past. *Progress in Human Geography, 31*, 638–653.
Hall, J., Arheimer, B., Borga, M., Brázdil, R., Claps, P., Kiss, A., et al. (2014). Understanding flood regime changes in Europe: A state-of-the-art assessment. *Hydrology and Earth System Sciences, 18*, 2735–2772.
Hanel, M., Vizina, A., Máca, P., & Pavlásek, J. (2012). A multi-model assessment of climate change impact on hydrological regime in the Czech Republic. *Journal of Hydrology and Hydromechanics, 603*, 152–161.
Hirschmuller, H. (2005). Accurate and efficient stereo processing by semi-global matching and mutual information. *Computer vision and pattern recognition, 2005. CVPR 2005. IEEE computer society conference on* (pp. 807–814). IEEE.
Jansky, B. (2006). Water retention in river basins. *Acta Universitatis Carolinae: Geographica, 38*, 173–184.
Kaiglová, J., Langhammer, J., Jiřinec, P., Janský, B., & Chalupová, D. (2015). Numerical simulations of heavily polluted fine-grained sediment remobilization using 1D, 1D+, and 2D channel schematization. *Environmental Monitoring and Assessment, 187*, 115.
Kliment, Z., Matoušková, M., Ledvinka, O., & Královec, V. (2011). Trend analysis of rainfall-runoff regimes in selected headwater areas of the Czech Republic. *Journal of Hydrology Hydromechahnics/Vodohospo. Cas, 59*, 36–50.
Kocum, J., & Janský, B. (2008). Possibilities of headwaters retention potential enhancement – case study upper Otava river basin. In B. M.Š. M (Ed.). *XXIVth conference of the danubian countries on the hydrological forecasting and hydrological bases of water management* (pp. 1–13). Presented at the Slovenian National Committee for the IHP UNESCO, Slovenian National Committee for the IHP UNESCO.
Kubinsky, D., Weis, K., Fuska, J., Lehotsky, M., & Petrovic, F. (2015). Changes in retention characteristics of 9 historical artificial water reservoirs near Banská Štiavnica, Slovakia. *Open Geosciences, 7*.
Kundzewicz, Z. W., Pińskwar, I., & Brakenridge, G. R. (2013). Large floods in Europe, 1985–2009. *Hydrological Sciences Journal, 58*, 1–7.
Křenová, Z., & Hruška, J. (2012). Proper zonation–an essential tool for the future conservation of the Šumava National Park. *European Journal of Environmental Sciences, 2*.
Langhammer, J., Su, Y., & Bernsteinová, J. (2015). Runoff response to climate warming and forest disturbance in a mid-mountain basin. *Water, 7*, 3320–3342.
Lindner, M., Maroschek, M., Netherer, S., Kremer, A., Barbati, A., Garcia-Gonzalo, J., et al. (2010). Climate change impacts, adaptive capacity, and vulnerability of European forest ecosystems. *Forest Ecology and Management, 259*, 698–709.
Matějková, I., van Diggelen, R., Prach, K., & Marrs, R. H. (2003). An attempt to restore a central European species-rich mountain grassland through grazing. *Applied Vegetation Science, 6*, 161–168.
Miřijovský, J., & Langhammer, J. (2015). Multitemporal monitoring of the morphodynamics of a mid-mountain stream using UAS photogrammetry. *Remote Sensing, 7*, 8586–8609.
Myeong, S., Nowak, D. J., Hopkins, P. F., & Brock, R. H. (2001). Urban cover mapping using digital, high-spatial resolution aerial imagery. *Urban Ecosystems, 5*, 243–256.
Nex, F., & Remondino, F. (2014). UAV for 3D mapping applications: A review. *Applied Geomatatics, 6*, 1–15.
NHI (2015). *National heritage catalog. 1000138018-Vchynice Tetov channel and reservoirs.* National Heritage Institute.
Papaioannou, G., Loukas, A., Vasiliades, L., & Aronica, G. T. (2016). Flood inundation mapping sensitivity to riverine spatial resolution and modelling approach. *Natural Hazards, 83*, 117–132.
Pepe, M., Fregonese, L., & Scaioni, M. (2018). Planning airborne photogrammetry and remote-sensing missions with modern platforms and sensors. *European Journal of Remote Sensing, 51*, 412–435.
Pepe, M., & Prezioso, G. (2016). Two approaches for dense DSM generation from aerial digital oblique camera system. *Proceedings of the 2nd international conference on geographical information systems theory, applications and management (GISTAM 2016)* (pp. 63–70). .
Räsänen, A., Nygren, A., Monge Monge, A., Käkönen, M., Kanninen, M., & Juhola, S. (2018). From divide to nexus: Interconnected land use and water governance changes shaping risks related to water. *Applied Geography, 90*, 106–114.
Raška, P., & Emmer, A. (2014). The 1916 catastrophic flood following the Bílá Desná dam failure: The role of historical data sources in the reconstruction of its geomorphologic and landscape effects. *Geomorphology, 226*, 135–147.
van Rees, E. (2015). *Creating aerial drone maps fast.* GeoInformatics.
Sampson, C. C., Smith, A. M., Bates, P. D., Neal, J. C., & Trigg, M. A. (2016). Perspectives on open access high resolution digital elevation models to produce global flood hazard layers. *Frontiers of Earth Science, 3*https://doi.org/10.3389/feart.2015.00085.
Šíma, J. (2013). Quality parameters of digital aerial survey and airborne laser scanning covering the entire area of the Czech Republic. *Geoinformatics FCE CTU, 10*, 15–26.
Sumava, N. P. (2016). *Vchynice-Tetov shipping canal.* Sumava National Park websitehttp://www.npsumava.cz/en/3129/3979/clanek/vchynice-tetov-shipping-canal/, Accessed date: 7 February 2018.
Tamminga, A. D., Eaton, B. C., & Hugenholtz, C. H. (2015). UAS-based remote sensing of fluvial change following an extreme flood event. *Earth Surface Processes and Landforms, 40*, 1464–1476.
Tansey, K., Chambers, I., Anstee, A., Denniss, A., & Lamb, A. (2009). Object-oriented classification of very high resolution airborne imagery for the extraction of hedgerows and field margin cover in agricultural areas. *Applied Geography, 29*, 145–157.
Thomas, I. A., Jordan, P., Shine, O., Fenton, O., Mellander, P.-E., Dunlop, P., et al. (2017/2). Defining optimal DEM resolutions and point densities for modelling hydrologically sensitive areas in agricultural catchments dominated by microtopography. *International Journal of Applied Earth Observation and Geoinformation, 54*, 38–52.
Turner, D., Lucieer, A., & Wallace, L. (2014). Direct georeferencing of ultrahigh-resolution UAV imagery. *IEEE Transactions on Geoscience and Remote Sensing, 52*, 2738–2745.
Turner, D., Lucieer, A., & Watson, C. (2012). An automated technique for generating georectified mosaics from ultra-high resolution unmanned aerial vehicle (UAV) imagery, based on structure from motion (SfM) point clouds. *Remote Sensing, 4*, 1392–1410.
Vlček, L., Kocum, J., Šefrna, L., Janský, B., & Kučerová, A. (2012). Retention potential and hydrological balance of a peat bog: Case study of Rokytka moors, otava river headwaters, sw. Czechia. *Geografie, 117*, 395–414.
Vozinaki, A.-E. K., Morianou, G. G., Alexakis, D. D., & Tsanis, I. K. (2017). Comparing 1D and combined 1D/2D hydraulic simulations using high-resolution topographic data: A case study of the koiliaris basin, Greece. *Hydrological Sciences Journal, 62*, 642–656.
Westoby, M. J., Brasington, J., Glasser, N. F., Hambrey, M. J., & Reynolds, J. M. (2012). “Structure-from-Motion” photogrammetry: A low-cost, effective tool for geoscience applications. *Geomorphology, 179*, 300–314.
Wohl, E. (2006). Human impacts to mountain streams. *Geomorphology, 79*, 217–248.